Mathematical and Computational Applications, Vol. 16, No. 4, pp. 868-878, 2011.

STRENGTHENING OF RC BEAMS WITH PREFABRICATED RC RECTANGULAR CROSS-SECTIONAL PLATES

M. Tekin[1], A. Demir[1], T. Turalı[1], H. Nohutçu[1], M. Bağcı[1]
[1]Department of Civil Engineering
Celal Bayar University, 45140
Muradiye, Manisa, Turkey
ali.demir@bayar.edu.tr

Abstract : The topic of this study is to strengthen cracked beams with prefabricated RC rectangular cross-sectional plates. The damaged beams were repaired by epoxy based glue. The repaired beams were strengthened using prefabricated RC rectangular cross-sectional plates. The strengthening plates were bonded to the bottom face of the beams by anchorage rods and epoxy. The strengthened beams were incrementally loaded up to maximum load capacities. The experimental results were satisfactory since the load carrying capacities of damaged beams were increased approximately 47% due to strengthening. The post-elastic strength enhancement and the displacement ductility of all the beams are researched during the experiments. The experimental program was supported by a three-dimensional nonlinear finite element analysis. The experimental results were compared with the results obtained from the beam modeled with ANSYS finite element program.

Keywords: Prefabricated RC plates, Strengthening, Load carrying capacity, Ductility, Epoxy, Anchorage rod, Finite element analysis

1. INTRODUCTION

Beams and columns of buildings or bridges that have been built long time ago or damaged due to an earthquake or other reasons are usually strengthened. In strengthening of beams, increasing the depth of a beam with a bonding plate is frequently used. For this reason, various techniques are proposed. The techniques used commonly in literature are to strengthen a beam by bonding steel plates [1, 2, 3]. Swamy et al. [4] researched the effect of glued steel plates on the first cracking load, cracking behavior, deformation, serviceability, and ultimate strength of RC beams. Adhikary and Mutsuyoshi [5] studied RC beams strengthened in shear with web-bonded continuous steel plates. Su et al. [6] investigated ductility performance of concrete beams under different bolt-plate arrangements. Instead of a steel plate, a FRP plate is also used in literature [7, 8, 9, 10, 11, 12]. Ceroni [13] researched RC beams externally strengthened with Carbon Fiber Reinforced Plastic (FRP) laminates and Near Surface Mounted (NSM) bars under monotonic and cyclic loads.
The experimental technique is necessary for reliable results, beside this; it should try to find a numerical method to solve the problem by computer. To do this, a finite element technique is used [14, 15, 16, 17]. In finite element analysis, discrete crack and smeared crack approaches are two major models representing cracking in concrete structures [18]. According to Ye [19], numerical results are dealing with flexural interfaces and nonlinear behavior of concrete have not been found in the literature.

In this study, the reference damaged beams were strengthened by prefabricated RC rectangular cross-sectional plates. The strengthening plates were bonded to the beams by epoxy based glue called “HILTI HIT-RE 500” and anchorage rods. The strengthened beams were incrementally loaded up to maximum load capacities. The results of the experiments were compared with the results obtained from the beam modeled with ANSYS nonlinear finite element program. It is thought that the strengthening method proposed can be useful, practical and reliable for a building or a bridge where similar beam sizes exist.

2. EXPERIMENTAL PROGRAM

2.1 Test setup

All beams were incrementally loaded up to maximum load capacities in order to define the load–displacement relationship. A single point bending test setup was adopted, as shown in Fig. 1. The beams were simply supported with the clear distance of 1800 mm between the supports and loaded at mid-span. Load was applied by a 250 kN hydraulic jack in the vertical direction. Mid-span displacements of beams were measured with the help of a linear variable displacement transducer (LVDT). The beam was incrementally loaded up to the failure under load control. For each increment of the load, the displacements were measured by the help of LVDTs placed at mid-span.

Figure 1. Reference RC beam

2.2 Specimen details

The reference beam size used was 150 mm (b) x 250 mm (h) x 2000 mm (l). Stirrups of 8 mm in diameter and 150 mm in interval were applied throughout the span of the beam.

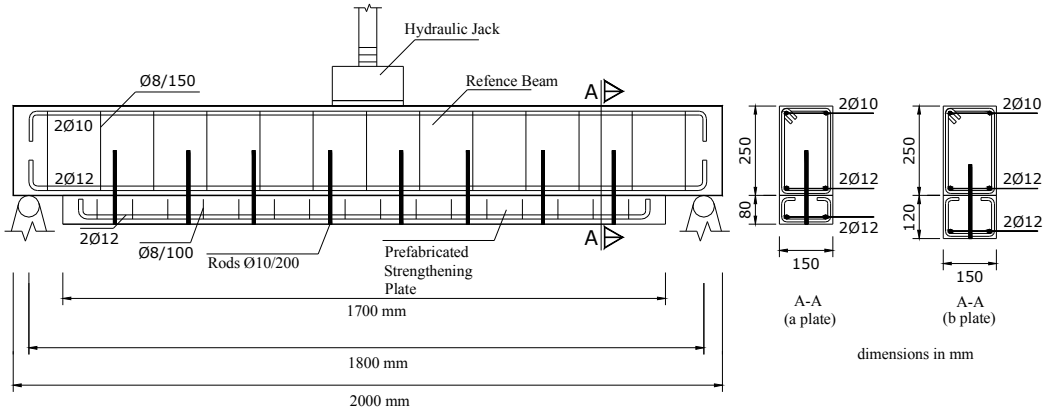

Figure 2. RC beams strengthened with prefabricated RC rectangular cross-sectioned plates

The reference beams named as “A1, A2” were reinforced with two Ø10 bars (10 mm in diameter) in the compression zone, two Ø12 bars (12 mm in diameter) in the tension zone, as shown in Fig. 1, Fig.2.
The rectangular cross-sectional prefabricated RC strengthening plates with 80 mm and 120 mm in thicknesses are named as “a1, b1”, respectively. The strengthening plates had been produced before they were bonded to the beams. The both strengthening plates were reinforced with two Ø12 bars (12 mm in diameter) in the tension zone. Stirrups of 8 mm in diameter and 100 mm in interval were applied as shown in Fig. 2.

2.3 Bonding procedure
The strengthening plates were bonded to the bottom face of the repaired beams by Hilti and anchorage rods. Before the anchorage rods of 10 mm in diameter and 200 mm in interval were applied, the holes of 12 mm in diameter on the bottom faces of the beams and strengthening plates were opened. These holes were filled by “Hilti”. The anchorage rods were driven about 150 mm into the holes, as seen in Fig.2, Fig.3.

Figure 3. The implementing of Hilti and anchorage rods

The reference beam A1 was strengthened by rectangular cross-sectional plates, as shown in Fig.2. The strengthening procedure of beam A2 was as beam A1. The reference beam, strengthening plate, anchorage rods were shown in Fig.2. The strengthened beams were loaded as in Fig.4.

Figure 4. Loading of strengthened beam

The cross-section and steel properties of the reference and strengthened beams, technical properties of epoxy were detailed in Table 1, Table 2, respectively.

Table 1. Properties of specimens

Specimens	Tension Bars	Stirrups (mm)	Depth (mm)	Width (mm)
A1	2Ø12	Ø8/150	250	150
a1	2Ø12	Ø8/100	80	150
A1a1	4Ø12	-	330	150
A2	2Ø12	Ø8/150	250	150
b1	2Ø12	Ø8/100	120	150
A2b1	4Ø12	-	370	150

Table.2 Technical properties of HILTI HIT-RE 500

Bond Strength ASTM C882-91[1]	12,4 MPa (7 day cure)
Compressive Strength ASTM D-695-96[1]	82,7 MPa
Compressive Modules ASTM D-695-96[1]	1493 MPa
Tensile Strength 7 day ASTM D-638-97	43,5 MPa
Base Materials	Concrete
Anchor Type	Chemical Anchor
Material Composition	Epoxy-adhesive
Base Material Temperature-range	-5°C-40°C

2.4 Material properties

A concrete mix containing maximum coarse aggregates of 10 mm was prepared. The cube strength of specimens was designed for 16 MPa at 28 days. The constituents and the corresponding proportions of the concrete mix were detailed in Table 3.

Table 3. Concrete mix adopted for producing a cubic meter of concrete

Unit	Water/Cement	Water	Cement	Fine aggregate	10 mm aggregate
kg/m^3	0,6	180	300	960	960

For each specimen, three concrete cubes with dimensions 150 mm x 150 mm x 150 mm were cast and compressive tests were carried out on the test day to obtain the compressive strength of cubes. The average concrete compressive strength of cubes was as shown in the Table 4.

Table 4. Test results of cube specimens

Specimens	Specimen Dimensions (mm)	Axial Load (kN)	Compressive Strength (MPa)
A1	150x150x150	442,8	19,68
a1	150x150x150	499,3	22,19
A2	150x150x150	349,4	15,53
b1	150x150x150	385,6	17,14

Three samples were taken from each type of reinforcement. The tensile tests were carried out and the yield strength and Young modulus of these samples were summarized in Table 5.

Table 5. Properties of reinforcements

Bar size (mm)	Young Modulus E_s (MPa)	Yield Strength (MPa)	Ultimate Strength (MPa)
8	210000	430	670
10	210000	425	660
12	210000	427	665

3. FINITE ELEMENT METHOD

In order to compare the experimental results, a nonlinear finite element model with ANSYS [20] was used to determine the ultimate load capacity of the beams. The properties and geometric characteristics of the beam in the nonlinear finite element model were taken the same as in the tested beams. Material properties of concrete and steel reinforcement in nonlinear finite element analysis are given below.

3.1 Concrete

In this study, Hognestad concrete model was used due to lack of confinement for the concrete [21]. The stress-strain values obtained from this model were used in the definition of the multilinear isotropic model. In the Hognestad concrete model, the part of stress strain curve until to the peak considered to be parabolic in the second degree; and the downward part considered to be linear. In the model, the formula for the parabola of the curve until the peak is given in Eq.(1) and for the maximum deformation in Eq.(2).

$$\sigma_c = f_c^{'}\left[\frac{2\varepsilon_c}{\varepsilon_{co}} - \left(\frac{\varepsilon_c}{\varepsilon_{co}}\right)^2\right] \quad (1)$$

$$\varepsilon_{co} = \frac{2f_c^{'}}{E_c} \quad (2)$$

The mechanical properties of concrete which were used in nonlinear finite element analysis were shown in Table 6. $f_c^{'}$ is the ultimate compressive strength of cylinder specimen; ε_{co} is the strain at the ultimate compressive strength $f_c^{'}$, ε_{cu} is the max strain, E_c is the modulus of elasticity of the concrete. The modulus of elasticity of concrete was taken as $4730\sqrt{f_c^{'}}$ (MPa) [22].

Table 6. Mechanical properties of concrete in nonlinear finite element analysis

Specimen	$f_c^{'}$ (MPa)	E_c (MPa)	ε_{co}	ε_{cu}	Poisson ratio
A1	16	19000	0,0017	0,003	0,2
a1	18	20000	0,0018	0,003	0,2
A2	13	17000	0,0015	0,003	0,2
b1	14	17700	0,0016	0,003	0,2

The Willam-Warnke failure model [23] used in the definition of the concrete. The Willam–Warnke failure model is used for modeling the failed collapsing surface of concrete without reinforcement under stress with three axes. If the calculated principle stress is more than the threshold stress, its behavior is considered to be nonlinear. In this case, the calculated principle stresses were used to determine the failure situation using the Willam–Warnke model. If Eq. (3) is obtained using these principals, it means that the stresses occur on the failure surface.

$$\frac{1}{\rho}\frac{\sigma_a}{f_c} + \frac{1}{r(\theta)}\frac{\tau_a}{f_c} = 1 \quad (3)$$

where σ_a and τ_a are average stress components, z is the apex of the surface and f_c is the uni-axial compressive strength, r is the position vector locating the failure surface with angle θ. The use of the Willam–Warnke mathematical model of the failure surface for the concrete has the advantages [10]: Close fit of experimental data in the operating range, Simple identification of model parameters from standard test data, Smoothness (continuous surface with continuously varying tangent planes).
Solid65 is used for the 3-D modeling of solids with or without reinforcing bars in ANSYS finite element program. The solid is capable of cracking in tension and crushing in compression. The element is defined by eight nodes having three degrees of freedom at each node: translations in the nodal x, y, and z directions [20].

3.2 Steel Reinforcement

The steel is a homogeneous and isotropic material which can be defined more easily and closer to reality than concrete. Unlike concrete, its properties do not depend on environmental conditions and time. Solid95 element is used in order to define the reinforcement that exist in ANSYS finite element program [20]. SOLID95 is a higher order version of the 3-D 8-node solid element SOLID45 which can tolerate irregular shapes without much loss of accuracy. SOLID95 elements have compatible displacement shapes and are well suited to model curved boundaries. The element is defined by 20 nodes having three degrees of freedom per node: translations in the nodal x, y, and z directions. The element may have any spatial orientation. SOLID95 has plasticity, creep, stress stiffening, large deflection, and large strain capabilities.
In this study, discrete modeling was used for reinforcement and stirrup steel in finite element analyses as seen in Fig. 5. The mechanical properties of steel which were used in the nonlinear finite element analysis were shown in Table 5.

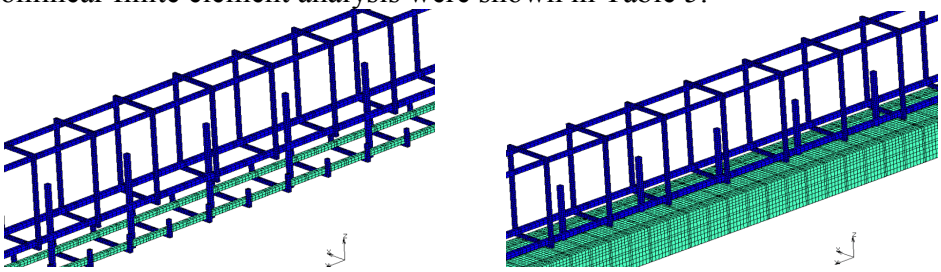

Figure 5. The models of reinforcements, stirrups and anchorage rods for strengthened beams

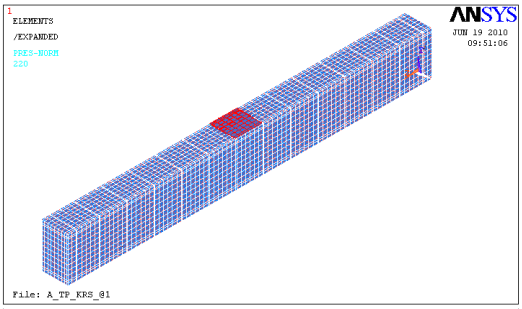

Figure 6. Finite element models of beams

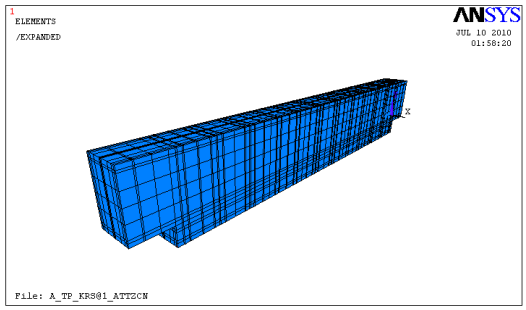

Figure 7. Finite element models of strengthened beams

A three-dimensional nonlinear finite element model and the typical finite element meshes of the reference beam and strengthened beam were shown in Fig.6, Fig.7.

4. EXPERIMENTAL AND FINITE ELEMENT RESULTS

The experimental and finite element results on the effect of prefabricated plates were presented and discussed in terms of the ultimate load, displacement, ductility, observed mode of failure.

4.1 Experimental strength and ductility

The reference beams A1, A2 were loaded until flexural cracks started to occur. These cracks were repaired with epoxy called "Hilti". The strengthening plates were bonded to the beams which were then loaded until they failed. It is observed that the beams A1, A2 cracked at 47,34 kN, 47,50 kN and the strengthened beams A1a1, A2b1 cracked at 70,14 kN, 69,40 kN load levels at the end of experimental loading, respectively. The load carrying capacity of strengthened beam A1a1 increased 48%. The load carrying capacity of strengthened beam A2b1 increased 46%. The experimental failure loads and increase in load carrying capacities were tabulated in Table 7.

Table 7. Experimental failure loads and capacity increases for reference and strengthened beams

Specimen	A1	A1a1	A2	A2b1
Experimental Failure Loads (kN)	47,34	70,14	47,50	69,40
Increase in Load Capacity due to Strengthening (%)	48		46	

The present experimental results indicated that the load-displacement curves of the beams, in Fig. 8, can be idealized by a bi-linear curve (Fig. 9). The displacement ductility factor μ_Δ, which is defined as the ratio between the displacement at peak load Δ_u and the notional yield displacement Δ_y is adopted to measure the ductility performance of the strengthened beams [6]. The displacement ductility factors of all beams were calculated using the above definitions and the results were tabulated in Table 8. The displacement ductility value of beam A1a1 was 2,186. The displacement ductility value of beam A2b1 was 2,347.

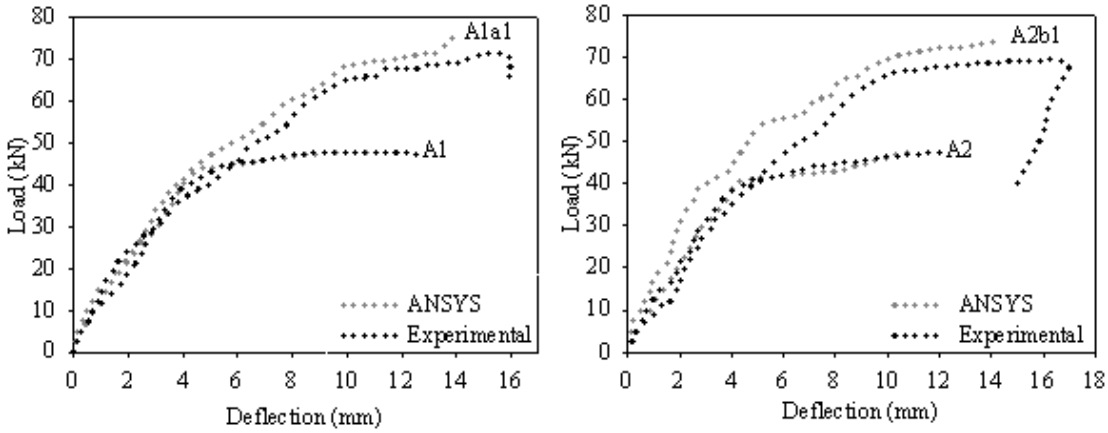

Figure 8. Comparison of experimental and ANSYS load–deflection curves for reference and strengthened beams

Substantial post-elastic strength enhancement could be found in Fig. 8. The post-elastic strength enhancement factor ν is defined as the ratio between the peak strength P_u and the yield strength P_y, see Fig. 9 [6]. The post-elastic strength enhancement factors of the beams were tabulated in Table 8. The post-elastic strength enhancement factor of beam A1a1 was 1,142. The post-elastic strength enhancement factor of beam A2b1 was 1,174.

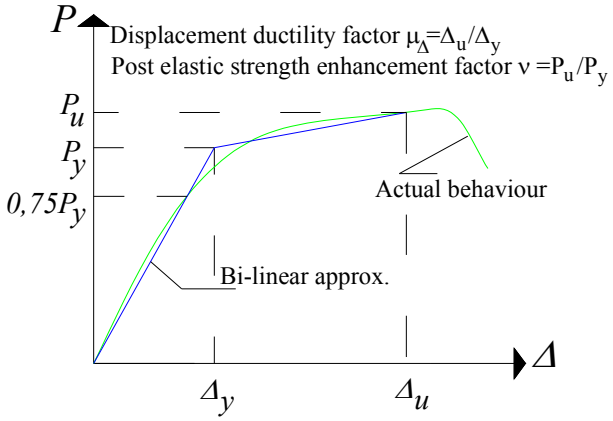

Figure 9. Definitions of displacement ductility factor and post-elastic strength enhancement factor for experiments

Table 8. Comparison of displacement ductility factors and post-elastic strength enhancement factors

Specimen	Δ_y (mm)	Δ_u (mm)	μ	P_y (kN)	P_u(kN)	ν
A1a1	7,32	16,00	2,186	61,40	70,14	1,142
A2b1	7,03	16,50	2,347	59,13	69,40	1,174

μ =displacement ductility, **ν**= the post-elastic strength enhancement factor

4.2 Failure Modes

The reference beams damaged by flexural cracks. The failure of strengthened beams had been associated with concrete cracking when the reinforcements in the beam yielded. The strengthening plates failed in shear during experiments. When the strengthened beams failed, capacities of the anchorage rods were not reached. The experimental failure processes of A1a1 and A2b1 were similar, as seen in Fig.10.

Figure 10. Concrete cracks of strengthened beams

4.3 Finite Element Results

The numerical ultimate failure loads and load versus mid-span displacement relationships were compared with the experimental results. The comparison of experimental and ANSYS results were given in Table 9. In the finite element analyses, point loads were applied at negative direction of y-axis as seen in Fig. 6, Fig.7. It was observed that the beams A1, A2 cracked at 47,87 kN, 48,10 kN and the strengthened beams A1a1, A2b1 cracked at 75,13 kN, 73,77 kN load levels at the end of finite element analyses, respectively.

The comparison of experimental and ANSYS load–mid-span displacement curves for reference and strengthened beams were given in Fig.8.

Table 9. Comparison for experimental and ANSYS results of reference and strengthened beams

Specimen	Experimental		ANSYS		Load Capacity Diff. %
	Load Capacity (kN)	Displacement (mm)	Load Capacity (kN)	Displacement (mm)	
A1	47,34	12,60	47,87	10,90	1,12
A1a1	70,14	16,00	75,13	13,90	7,11
A2	47,50	12,00	48,10	11,10	1,26
A2b1	69,40	16,50	73,77	14,10	6,29

The stress distribution and cracks of beam A1a1 in nonlinear finite element analysis were shown in Fig.11. Experimental and ANSYS failure processes of A1a1 and A2b1 were similar. The both of the strengthened beams were failed with shear cracks during the experiments.

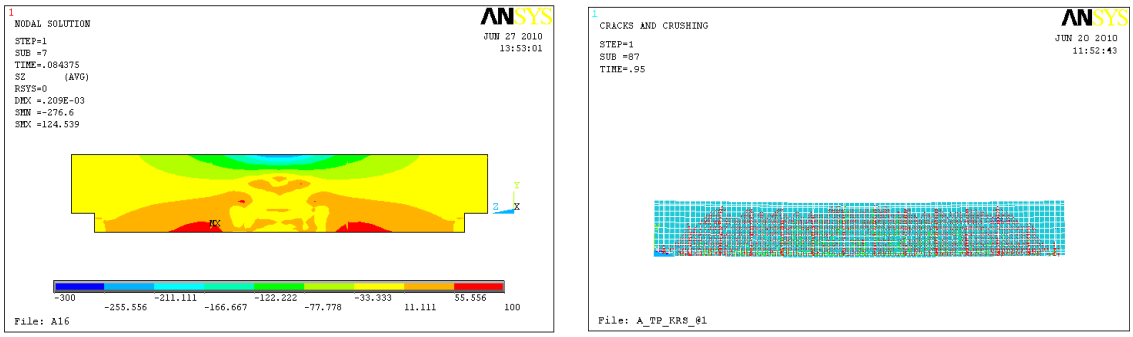

Figure 11. Stress distribution and cracks of strengthened beam A1a1

4. CONCLUSIONS

There are several strengthening methods found in the literatures which use FRP plates or steel plates. But, corrosion is important problem for steel plates. Although FRP plates are safe and light in weight, fire and freeze-thaw are important problems for them. Moreover, strengthening with FRP and steel plates, the structure does not get extra strength against lateral loads. Therefore a new strengthening method for structural

beams is proposed in this study. In this method, the lateral load carrying capacity increases since the depth of the beams increase. In addition the moment capacities of the beams are increased. Since the strengthening plate is made of the same material as the beams, it is more aesthetic and economic. It increases the rigidity of the beam whereas this is not the case in other methods. The strengthening method proposed is a good alternative to strengthening with FRP and steel plates.

The post-elastic strength enhancement and displacement ductility are identified as two important structural performance criteria for structures predominantly subjected to gravity loads. These two criteria are influenced by the prefabricated strengthening plates. It was observed that sufficient displacement ductility and sufficient strength enhancement could be achieved by the rectangular cross-sectional plates.

The comparison of experimental and ANSYS load–displacement curves for reference and strengthened beams were shown in Fig.8. It is seen that the experimental cracking loads obtained for the beams were close to the results obtained for the same beams by ANSYS computer program. The experimental technique is necessary for reliable results; moreover one should try to find a numerical method to solve the problem by computer. To achieve this end, a finite element technique is used. In the finite element method, the Hognestad model for stress-strain diagram of concrete is used whereas in the experimental method the actual stress-strain diagram of the concrete is used. For this reason, the load-displacement differences between the experimental and the finite element method are found.

Due to the reasons mentioned above it can be said that the strengthening method examined both experimentally and numerically is practical, reliable and economic. More experimental and theoretical studies are recommended for the better determination behavior of strengthened beams with prefabricated RC plates.

Acknowledgements

The research described here was supported by the Scientific Research Project Commission of Celal Bayar University (Project No. Muh2007-22). The generous support of the construction materials by Manisa ER Prefabricated Corporation is gratefully acknowledged.

REFERENCES

1. Swamy R.N., Jones R. and Charif A. (1989a). The effect of external plate reinforcement on the strengthening of structurally damaged RC beams. Structural Engineer, 67(3): 45-56.

2. Barnes R.A., Baglin P.S., Mays G.C., Subedi N.K. (2001). External steel plate systems for the shear strengthening of reinforced concrete beams. Engineering Structures, 23:1162-1176.

3. Arslan G., Sevuk F., Ekiz I. (2008). Steel plate contribution to load-carrying capacity of retrofitted RC beams. Construction and Building Materials, 22:143-153.

4. Swamy R.N., Jones R., Bloxham J.W. (1987b). Structural behaviour of reinforced concrete beams strengthened by epoxy-bonded steel plates. Structural Engineer, 65(2):59-68.

5. Adhikary B.B., Mutsuyoshi, H. (2006(. Shear strengthening of RC beams with web-bonded continuous steel plates. Construction and Building Materials, 20:296-307.
6. Su, R.K.L., Siu W.H., Smith S.T. (2010). Effects of bolt plate arrangements on steel plate strengthened reinforced concrete beams. Engineering Structures, 32:1769-1778.
7. El-Mihilmy M.T. and Tedesco, W.J. (2000). Analysis of reinforced concrete beams strengthened with FRP laminates. Journal of Structural Engineering, (ASCE)126(6): 684-691.
8. Buyukozturk, O. and Karaca, E. (2002). Characterization and modeling of debonding in RC beams strengthened with FRP composites. In: Proceedings 15.ASCE Engineering Mechanics Conference, 2-5 June 2002. Columbia Univ., New York, N.Y.
9. Lu X.Z., Teng J.G., Ye L.P. and Jiang J.J. (2005). Bond-Slip Models for FRP Sheets/Plates Bonded to Concrete. Engineering Structures, 27(6):920-937.
10. Ozcan M., Bayraktar A., Sahin A., Haktanır T., Turker T. (2009). Experimental and finite element analysis on the steel fiber reinforced concrete (SFRC) beams ultimate behavior. Construction and Buildings Materials, 23:1064-1077.
11. De Lorenzis, L. and Teng, J. G. (2007). Near-Surface Mounted FRP Reinforcement: An Emerging Technique for Strengthening Structures. Composites Part B: Engineering, 38(2): 119-143.
12. Eshwar N., Nanni A., and Ibell T.J. (2004). Effectiveness of CFRP Strengthening on Curved Soffit RC Beams. Advances in Structural Engineering, 8(1):55-68.
13. Ceroni F. (2010). Experimental performances of RC beams strengthened with FRP materials. Construction and Building Materials, 24:1547–1559.
14. Barbosa A.F. and Ribeiro G.O. (2004). Analysis of reinforced concrete structures using ANSYS nonlinear concrete model. Computational Mechanics, 1(8):1-7.
15. Pham H., Al-Mahaidi R., Sauma V. (2006). Modeling of CFRP concrete bond using smeared and discrete cracks. Composite Structures, 75:145-150.
16. Hawileh R.A., Naser M., Zaidan W., Rasheed H.A. (2009). Modeling of insulated CFRP-strengthened reinforced concrete T-beam exposed to fire. Engineering Structures, 31:3072-3079.
17. Buyukkaragoz, A. (2010). Finite element analysis of the beam strengthened with prefabricated reinforced concrete plate. Scientific Research and Essays, 5(6):533-544.
18. Yang ZJ, Chen JF, Proverbs D. (2003). Finite element modeling of concrete cover separations failure in FRP plated beams. Construct Build Mater, 17(1):3–13.
19. Ye JQ. (2001). Interfacial shear transfer of RC beams strengthened by bonded composite plates. Cem Concr Comp, 23(4–5):411–7.
20. ANSYS. (2007). Finite element computer program. Version 11. Canonsburg (PA): ANSYS, Inc.
21. Hognestad E. (1951). A study of combined bending and axial load in RC members. Univ. Illinois Eng. Exp. Stat. Bull, 399(2):36-57.
22. ACI Committee 318. Building code for structural concrete (318R- 2002) and commentary (318R-2002). ACI, Farmington Hills, MI, 2002.
23. Willam K.J. and Warnke E.P. (1974). Constitutive model for triaxial behavior of concrete. In: Proceedings of the International association of bridge and structural engineering conference 1974; 174-191.